



Compression of a Spherically Symmetric DT Plasma Liner onto a Magnetized DT Target

J.F. Santarius

March 2012

UWFDM-1409

Submitted to *Physics of Plasmas*.

FUSION TECHNOLOGY INSTITUTE
UNIVERSITY OF WISCONSIN
MADISON WISCONSIN

**Compression of a Spherically Symmetric DT
Plasma Liner onto a Magnetized DT Target**

J.F. Santarius

Fusion Technology Institute
University of Wisconsin
1500 Engineering Drive
Madison, WI 53706

<http://fti.neep.wisc.edu>

March 2012

UWFDM-1409

Submitted to *Physics of Plasmas*.

Abstract

Converging plasma jets can form warm dense matter (WDM) and may be able to reach the regime of high energy density plasmas (HEDP). The successful application of plasma jets to magneto-inertial fusion (MIF) would heat the plasma by fusion products and should increase the plasma energy density. This paper reports the results of using the University of Wisconsin's 1-D Lagrangian, radiation-hydrodynamics, fusion code BUCKY to investigate two MIF converging plasma jet test cases originally analyzed by R. Samulyak, P. Parks, and L. Wu [*Physics of Plasmas* **17**, 092702 (2010)]. In these cases, 15 cm or 5 cm radially thick deuterium plasma jets merge at 60 cm from the origin and converge radially onto a magnetized target of radius 5 cm. The BUCKY calculations reported here, starting at the time of impact of the plasma jets on the target, model the compression and expansion of deuterium-tritium plasma jets with the same mass density and thickness. One-temperature and two-temperature BUCKY results differ considerably for the thicker liner case, reflecting the sensitivity of the calculations to details of the timing and plasma parameters. Compared to Samulyak, et al., the BUCKY code results showed similar behavior of the plasma, except for a much longer dwell time near maximum compression.

I. INTRODUCTION

The well documented importance of high energy density plasmas (HEDP)^{1,2,3,4,5} motivates investigating the use of plasma jets to form HEDP. An intriguing possibility is that the leverage of fusion-product heating might generate plasmas of even higher energy density through magneto-inertial fusion (MIF). Often called magnetized-target fusion (MTF), MIF constitutes one potential option for pulsed power generation of electricity.⁶ The MIF path to HEDP grew out of the pinch program, which was—along with stellarators and magnetic mirrors—one of the earliest avenues of fusion investigation,⁷ and out of pulsed magnetic field generation research.⁸ Pulsed power concepts seek to implode a plasma to high temperature and confine it for times sufficiently long to produce substantial fusion energy.

In MIF, a converging, initially solid, liquid, or plasma external conductor implodes a magnetized plasma through inertia and magnetic flux conservation.^{9,10} The MIF concept relies on the magnetic field of the target to reduce thermal conduction and on the liner's inertia to facilitate transient plasma stability and confinement. The early MIF research focused on solid or liquid liners. Scientists performed a modest amount of MIF research during the 1980s and early 1990s.¹⁰ In the mid-to-late 2000s, MIF research benefited particularly by collaborations on an MIF proof-of-principle experiment,¹¹ led by Los Alamos National Laboratory (LANL) and the Air Force Research Laboratory (AFRL). This also stimulated related research,^{12,13,14} including successful experiments on imploding solid liners¹⁵ and creating a suitable field-reversed configuration (FRC) for the target.^{16,17}

The idea of replacing the solid or liquid liner with plasma jets was invented in the late 1990s.^{18,19} The advantage of plasma liners over solid or liquid liners for MIF is the ability of plasma guns to produce plasma jets that reach very high velocities while a sufficient standoff distance protects the guns from the fusion blast. One key aspect of merging plasma jets has been tested successfully in cylindrical geometry at moderate energy (24 kJ plasma guns) at AFRL,²⁰ and HyperV Corporation also has an active experimental program in this area.²¹

This paper reports 1-D radiation hydrodynamics calculations that use a Lagrangian computer code to simulate the compression and fusion burn for cases closely related to two cases computationally evaluated in Ref. 22, which in turn were based on a theoretical analysis developed in Ref. 23. This paper will not address plasma instabilities, which require a higher-dimensional analysis.

II. COMPUTATIONAL APPROACH

The University of Wisconsin's BUCKY computer code^{24,25} serves as the workhorse computational tool for much of the UW's pulsed power plasma physics research, including MIF, Z-pinch,²⁶ and inertial-confinement fusion (ICF).²⁷ BUCKY is a 1-D, Lagrangian, radiation-hydrodynamics fusion code that can simulate plasmas in planar, cylindrical, or spherical geometries. It solves single-fluid equations of motion with pressure contributions from electrons, ions, radiation, and fast charged particles. Plasma energy transfer can be treated using either a one-temperature ($T_e=T_i$) or two-temperature model. In the latter case, the electrons and ions are assumed to have Maxwellian distributions defined by T_e and T_i . The temperature

equations are coupled by an electron-ion energy exchange term and each equation has a PdV work term. The BUCKY code uses equation-of-state and opacity lookup tables. For the present calculations, a computational procedure that solves rate equations for detailed atomic models as described in Ref. 28 was used to generate the tables. In addition to radiation, BUCKY includes heating due to the deposition of fast charged particles and neutrons during the fusion burn phase. Fusion burn equations from D-T, D-D, and D-³He reactions are solved, and the charged-particle reaction products are transported and slowed using a time-dependent, particle-tracking algorithm. Neutrons are deposited in the target using an escape probability model. Fast-ion fusion products and target microexplosion debris are tracked using either local deposition or a time-, energy-, and species-dependent stopping power model. Stopping powers are computed using a Lindhard model at low projectile energies and a Bethe model at high energies.

The BUCKY code and related Mathematica[®] pre- and post-processor notebooks for the BUCKY results have been modified in several ways to address MIF physics:

1. Added magnetic-field enhanced Braginskii perpendicular thermal conductivities²⁹ for the electrons (subscript e) and ions (subscript i):

$$\kappa_{\perp e} = \frac{n_e k(kT_e) \tau_{ee}}{m_e} \left(\frac{4.66 \omega_{ce}^2 \tau_{ee}^2 + 11.92}{\omega_{ce}^4 \tau_{ee}^4 + 14.79 \omega_{ce}^2 \tau_{ee}^2 + 3.77} \right) \quad (1)$$

$$\kappa_{\perp i} = \frac{n_i k(kT_i) \tau_{ii}}{m_i} \left(\frac{2 \omega_{ci}^2 \tau_{ii}^2 + 2.64}{\omega_{ci}^4 \tau_{ii}^4 + 2.7 \omega_{ci}^2 \tau_{ii}^2 + 0.68} \right) \quad (2)$$

where k is Boltzmann's constant, m is mass, n is density, T is temperature, τ is 90° scattering collision time, and ω_c is cyclotron frequency.

2. Added magnetic flux conservation during magnetized target compression to BUCKY. Because BUCKY is a 1-D code, a pseudo-spherical magnetic field with conserved $r^2 B$ was invoked. The physics basis for this assumption has been demonstrated for ICF capsules at the Laboratory for Laser Energetics.³⁰ This assumption should model the electron heat transport and magnetic pressure reasonably well, but end effects remain to be assessed.
3. Developed a Mathematica[®] notebook to calculate appropriate MIF input case parameters for the BUCKY code. This notebook calculates various quantities and, in particular, assures that the masses of contiguous Lagrangian zones differ by no more than 2%. This notebook also calculates initial zone masses and radii that model a given radial density profile.

One key objective of the seminal analysis of plasma-jet MIF was the enhancement of the burn time by extending the compressed-target phase using the inertia of a massive liner (outer radial zones).¹⁸ An approach to analyzing simple test cases for this problem has been published in Refs. 22 and 23. The main objective of the present paper is the comparison of BUCKY calculations to two computational cases of Ref. 22.

Because the BUCKY code uses equation-of-state table lookup and a DT table generated by the UW EOSOPA code³¹ was available, the analysis described in this paper uses DT fuel instead of the pure deuterium fuel of Ref. 22, but it maintains the same mass density initial profile. The

Ref. 22 cases generate total fusion energies that are very much smaller than the input kinetic energy of the plasma jets, so the increased fusion energy generated by the larger DT fusion cross section compared to DD should not significantly alter the results.

III. TEST CASES

The Samulyak, Parks, and Wu²² (hereafter SPW) paper reported one-temperature radiation hydrodynamics calculations that used the numerical method of front tracking^{32,33} and discussed several cases. The two cases of Reference 22 treated here model pure deuterium, spherically converging plasma jets, initially of 15 cm or 5 cm thickness, that merge at 60 cm from the origin into a spherically symmetric liner of mass density= 3.8×10^{-5} g cm⁻³, temperature=0.0358 eV, and velocity=100 km s⁻¹. At impact of the liner, the magnetized DD plasma target has an initial magnetic field=2 T, radius=5 cm, mass density= 8.3×10^{-6} g cm⁻³, temperature=100 eV, and ratio of specific heats=5/3. The Fig. 3 of SPW shows a calculation of the mass density as a function of radius for the liner at the initial moment of impact with the target. Because of the difficulty of following the liner through the vacuum region between it and the target using a Lagrangian code such as BUCKY, the computational results shown in this paper's Sec. IV start from this SPW radial profile of the mass density. The 15 cm initial thickness liner case of SPW is redrawn from Ref. 22, Fig. 3 as the curve labeled " $\Delta_{\text{liner}}=0.15$ m" in Figure 1.

In the SPW paper's other case treated in this paper, the deuterium liner thickness is reduced to 5 cm at the 60 cm merging radius and the other parameters are kept the same as in the 15 cm case. The liner mass is thereby reduced by a factor of 3.5, and the kinetic energy is decreased by the same factor as compared to the 15 cm case. For the 5 cm thick liner BUCKY calculations, the SPW radial density profile of their 15 cm thick liner case has been scaled by keeping the liner masses the same for the 5 cm case SPW and BUCKY cases. The resulting 5 cm initial thickness liner case radial density profile also appears in Figure 1.

The key input parameters for the present computations appear in Table 1, where, for each region (target or jets), ξ is the ratio of the mass of zone $i+1$ to the mass of zone i , Δ is the region thickness, r is the zone outer radius, m is the total mass, ave. ρ is the average mass density, T_e is the electron temperature, v is the initial zone velocity, M is the Mach number, and KE is the total kinetic energy.

For the 15 cm initial thickness liner case (solid red), labeled " $\Delta_{\text{liner}}=0.15$ m", the calculation used the profile given in Ref. 22, redrawn here from SPW, Fig. 3. For the 5 cm initial thickness liner case, labeled " $\Delta_{\text{liner}}=0.05$ m", the density profile was extrapolated from the 15 cm case profile, as discussed in Sec. III.

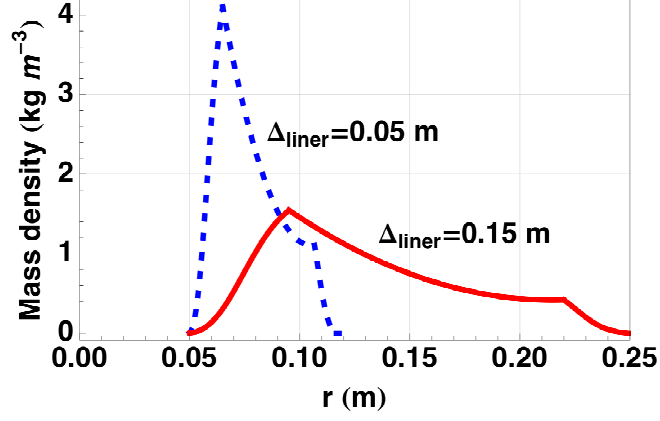


Figure 1. Liner mass density profile at impact with the target used for the BUCKY calculations.

Table 1. Key MIF parameters for the SPW 15 cm initial thickness liner case BUCKY input (DT target and jets).

	Target	Jets
# of zones	200	500
ξ	1	1.02
Δ (m)	0.05	0.20
r (m)	0.05	0.25
m (g)	0.0043	32
ave. ρ (kg m^{-3})	0.0083	0.49
T_e (keV)	100	0.036
v (km/s)	0	100
M	0	70
KE (MJ)	0	160

IV. RESULTS

A. Comparison to Samulyak, Parks, and Wu 15 cm deuterium liner case

1. One-temperature BUCKY calculation of 15 cm liner case

The results of running BUCKY to simulate the SPW 15 cm initial thickness liner case appear in Figs. 2-9 and Table 2. Figure 2 shows r-t plots of the Lagrangian constant-mass zones for the convergence and expansion of the plasma liner and target for: (a) the full extent of the initial target and jet plasma zones, and (b) the near-axis plasma. Figure 3 plots the positions of the liner-target interfaces predicted by this BUCKY calculation and Ref. 22's front tracking-code; the BUCKY result shows a much longer dwell time than does the SPW calculation. The BUCKY calculation's behavior qualitatively agrees with Ref. 18 and a recent paper that predicts plasma jet parameters can be chosen to give a "bounce-free" (very long dwell time) implosion.³⁴

Figure 4 illustrates the detailed time evolution of all zones for the DT reaction rate, total pressure, fluid velocity, plasma temperature, average charge state, and mass density. As the DT reaction rate and total pressure plots of Figure 4 illustrate, the BUCKY code predicts that for this case the DT reaction rate and peak pressure are approximately synchronous and remain near their peak values for a few tenths of a μs . The peak plasma temperature of 8.8 keV occurs in the innermost target zone, and the average target plasma temperature is 2.3 keV. These values are slightly below the SPW peak temperature of over 10 keV and average temperature of 5.2 keV.

One key question of magneto-inertial fusion is how long the plasma target remains compressed, the so-called "dwell time", sometimes characterized by the time for the radius and pressure to rise to twice the radius or half the pressure of their values at maximum compression. These times, radii, and pressures for the BUCKY calculations of the SPW 15 cm initial thickness liner case appear in Table 2. Note that a steep change in pressure with time necessitates interpolation due to the BUCKY code's output occurring at discrete intervals, although the half-pressure time can be bracketed to within 0.1 μs . As Figure 3 illustrates, the BUCKY code predicts that the target remains highly compressed for about 2 μs , and the approximate measure, listed in Table 2, is that it takes 2.25 μs to reach twice the radius at maximum compression, whereas SPW predict $\sim 0.22 \mu\text{s}$ for this to happen. The calculated minimum interface radius is similar in both cases, 0.62 cm for BUCKY and 0.73 cm for SPW, as is the target-liner interface's asymptotic expansion velocity, 0.77 $\mu\text{s cm}^{-1}$ for BUCKY and 0.58 $\mu\text{s cm}^{-1}$ for SPW. Both codes predict roughly equal times for the interface zone to go from maximum to half-maximum pressure: 0.26 μs for the BUCKY code and 0.22 μs for SPW. The BUCKY code predicts a peak pressure at the interface of 14 Mbar compared to 11 Mbar for SPW.

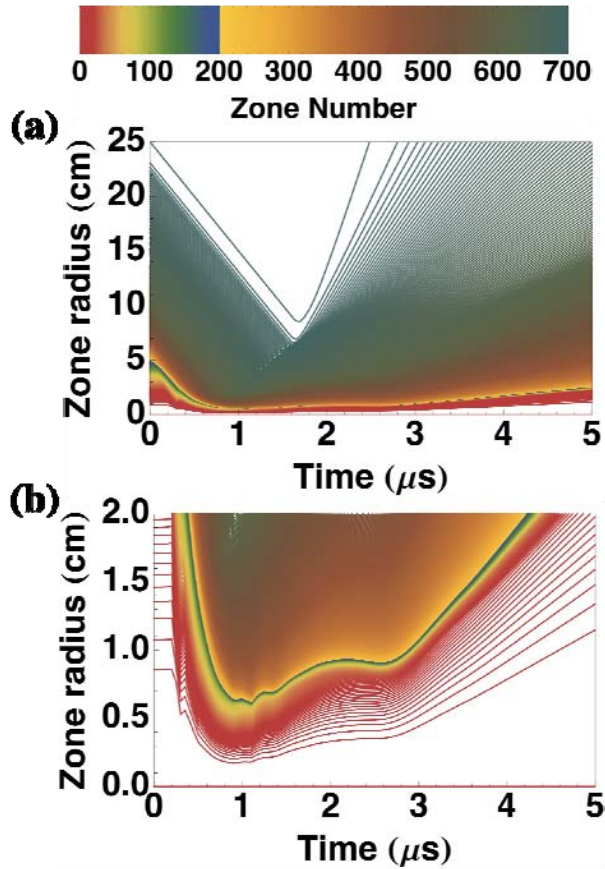


Figure 2. Lagrangian (constant mass) zone radii versus time for the BUCKY DT plasma-jet MIF calculation of the 15 cm initial thickness liner case of Ref. 22: (a) $r < 25$ cm and (b) near-axis zones, $r < 2$ cm. Target zones 1-200 use the dark rainbow colors of Mathematica[®], and liner zones 201-700 use the fall colors. All subsequent Lagrangian zone plots in this paper use this color scheme.

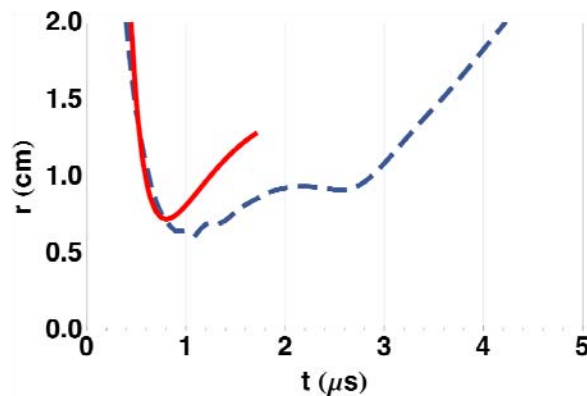


Figure 3. Calculations of the BUCKY code (dashed blue) and the Ref. 22 front-tracking code (solid red) for the location of the interface between the liner and the target as a function of time for the 15 cm initial thickness liner case. The SPW (Ref. 22) times have been shifted to match approximately the slopes of the curves as the plasma jets move inwards.

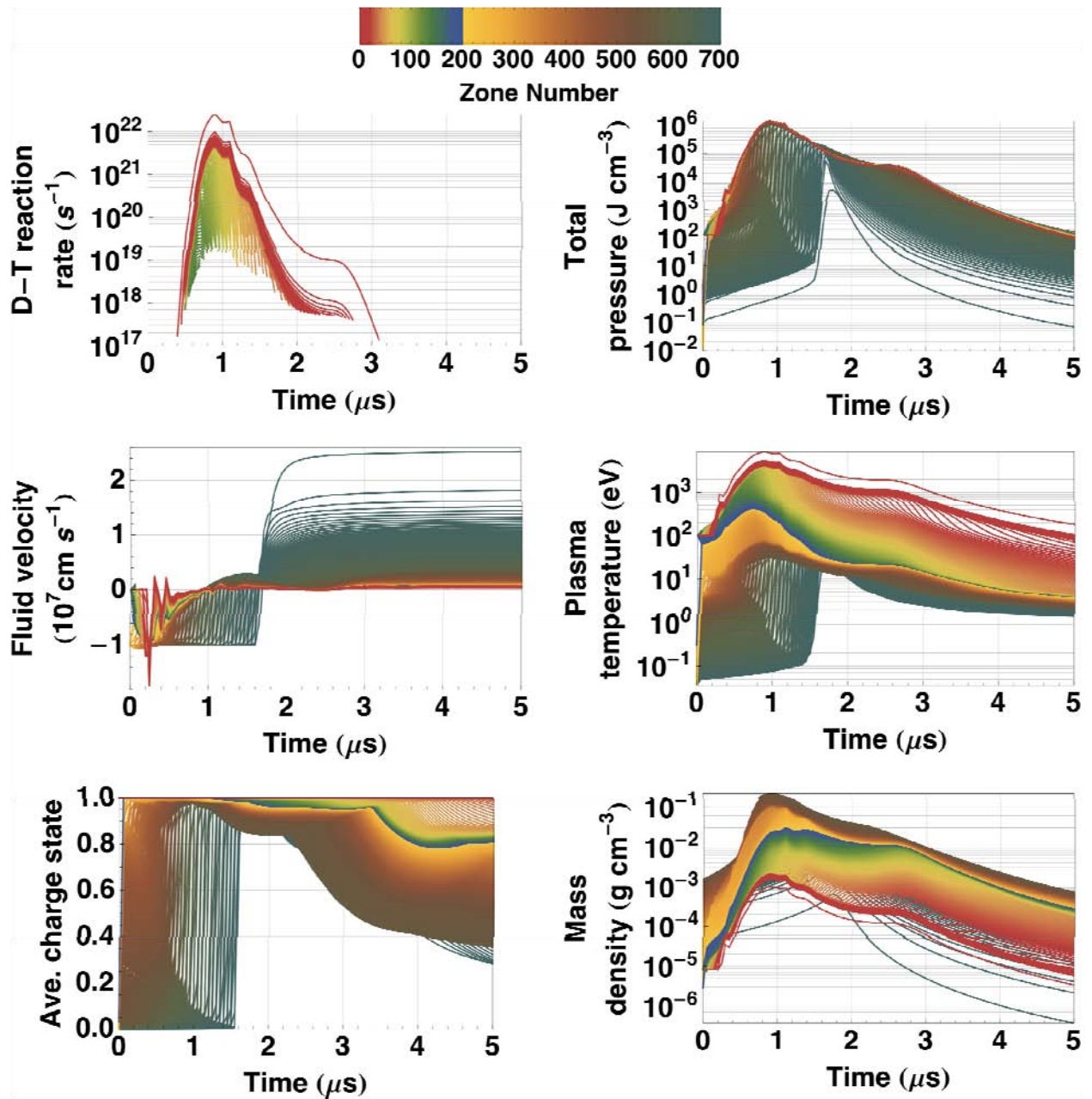


Figure 4. Selected zone parameters vs. time for the BUCKY DT plasma-jet MIF calculation of the 15 cm initial thickness liner case of Ref. 22.

Table 2. Time for the liner-target interface to reach (a) twice the radius or (b) half the pressure of the value at maximum compression for the BUCKY run of the SPW 15 cm initial thickness liner case. The Δt for half pressure is an extrapolated value that is bracketed within 0.1 μs .

(a)		Time	Radius
		(μs)	(cm)
	Min. r	1.1	0.62
	Twice r	3.25	1.27
	Δt	2.15	
(b)		Time	Pressure
		(μs)	(J cm^{-3})
	Max. P	0.90	1.45×10^6
	Half P	1.16	0.72×10^6
	Δt	0.26	

2. Two-temperature BUCKY calculation of 15 cm liner case

The results of performing a two-temperature calculation instead of the one-temperature calculation of Sec. A.1 and SPW for the 15 cm liner case, when running otherwise the same input parameters, appear in Figures 5-9. In comparison with the r-t plot versus time of the one-temperature BUCKY calculation (cf. Figure 2b), the two-temperature result in Figure 5 shows slightly more compression and a much longer dwell time near maximum compression for zones near the axis. Zones at larger radii show little difference between the 1-T and 2-T calculations.

The 2-T calculation zone parameters shown in Figure 6 and Figure 7 indicate that the core plasma stays somewhat cooler than in the 1-T case (cf. Figure 4), but the mass density is higher and varies more among the target zones. The net effect is reduced plasma pressure and fusion rates for the 2-T case. The ion-electron temperature difference ($T_e - T_i$) for all zones vs. time for the first 2 μs of the 2-T simulation, which contains all significant temperature differences, appears in Figure 7. The zone fluid velocities vary little between the 1-T and 2-T cases.

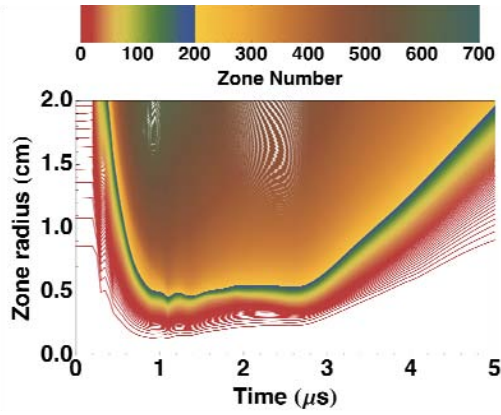


Figure 5. Lagrangian zone radii versus time of the near-axis zones for a two-temperature, BUCKY DT plasma-jet MIF calculation of the 15 cm initial thickness liner case.

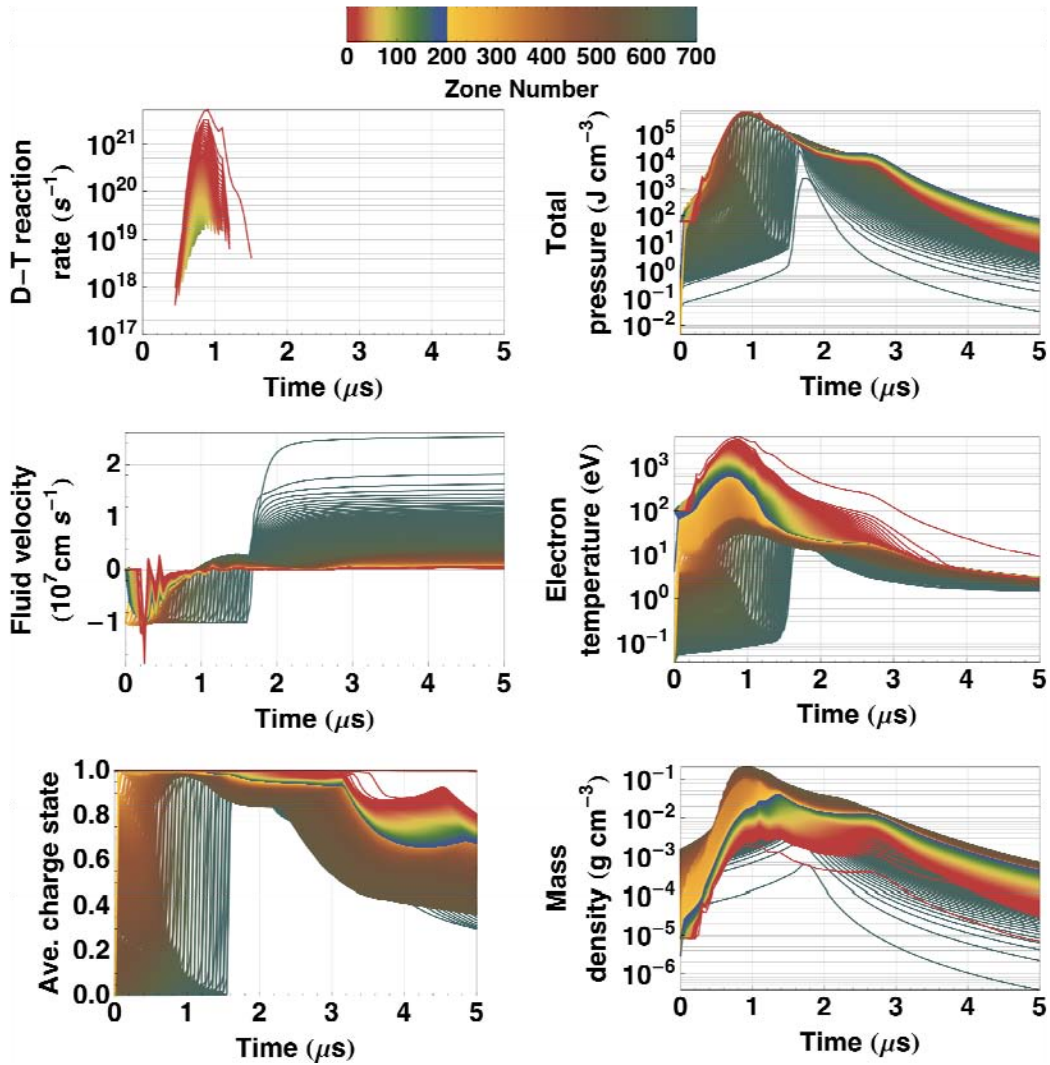


Figure 6. Selected zone parameters vs. time for the two-temperature BUCKY DT plasma-jet MIF calculation of the 15 cm initial thickness liner case.

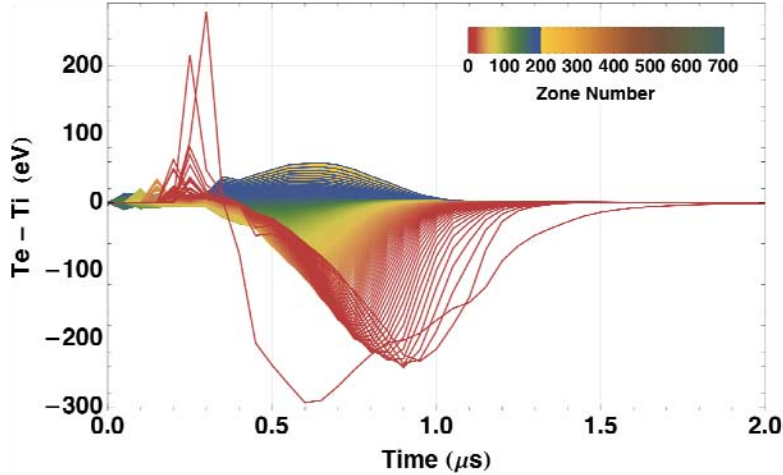


Figure 7. Electron-ion temperature difference for the first two μs of the BUCKY calculations of the SPW 15 cm initial thickness liner case.²²

3. Comparison of 1-T and 2-T BUCKY calculations for the 15 cm liner case

The cumulative fusion energy and the magnetic field in the target as a function of time for the 1-T and 2-T BUCKY calculations of the 15 cm liner case appear in Figure 8. Figure 8 shows the cumulative fusion energy and indicates that the energy essentially all gets produced within a few tenths of a μs in both cases. Despite the longer dwell time of the plasma near the axis for the 2-T case (cf. Figure 2 and Figure 5), the 1-T case's fusion yield is much larger. The 2-T case's peak magnetic field is about twice that of the 1-T case. Figure 9 plots the average target mass density and ion temperature vs. time for the 1-T and 2-T calculations.

The 1-T case's higher ion temperature and better correlation of maximum density with maximum temperature appear to lead to that case's higher fusion yield. The differences in zone parameter evolution shown in Figure 4 and Figure 6, although relatively small, may alter the shock timing and detailed parameter evolution sufficiently to change the fusion yield significantly. Testing whether this trend continues for cases beyond the two SPW cases treated in this paper awaits the running of further cases and the exploration of parameter space in depth.

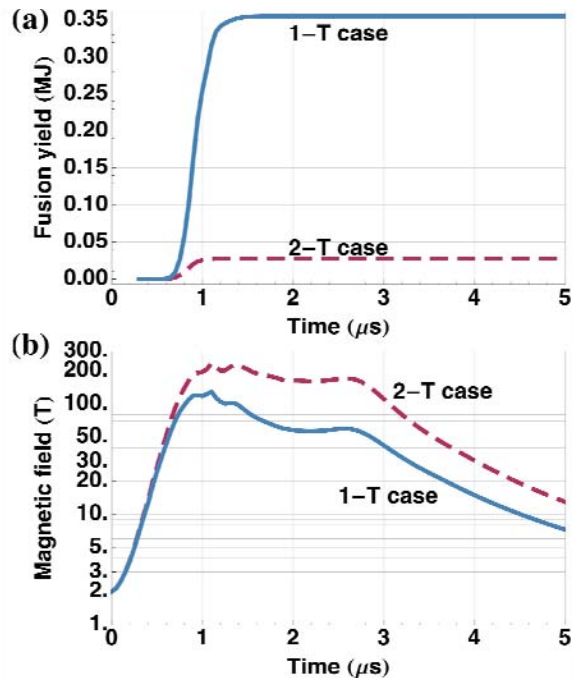


Figure 8. (a) Cumulative fusion energy yield and (b) magnetic field vs. time for BUCKY 1-T (solid blue) and 2-T (dashed maroon) calculations of the SPW 15 cm initial thickness liner case.²²

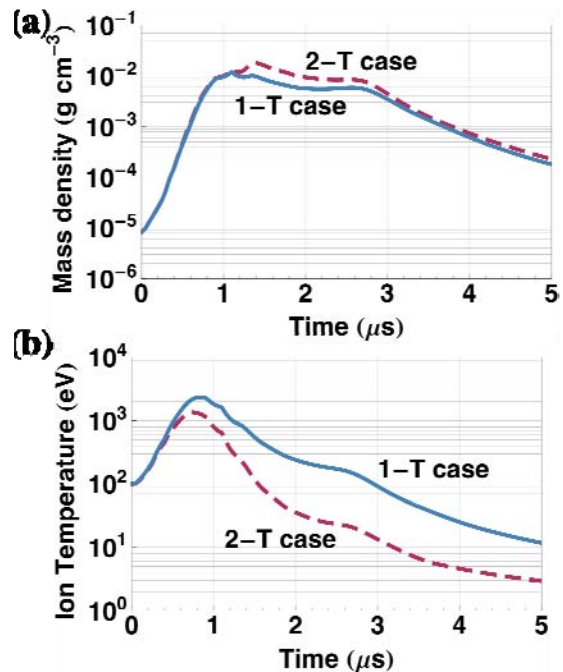


Figure 9. Average (a) mass density and (b) ion temperature vs. time for the target regions for BUCKY 1-T (solid blue) and 2-T (dashed maroon) calculations of the SPW 15 cm initial thickness liner case.²²

B. Comparison to Samulyak, Parks, and Wu 5 cm DD liner case

For the BUCKY calculations that simulate the SPW 5 cm liner case, the plasma density radial profile was extrapolated from the merging time to the time of target impact, as discussed in Sec. III. This makes the results of this section more approximate than those for the 15 cm case, where SPW provided a plot of the radial plasma density at the time of target impact. Nevertheless, the qualitative features of the results given in this section should remain reasonably accurate.

The BUCKY results for the 5 cm liner case appear in Figs. 10-13. Figure 10a shows all Lagrangian zones, and the near-axis behavior appears in Figure 10b. Comparing against the evolution of the liner-target interface for the 15 cm case, as shown in Figure 2 and Figure 3, indicates that the BUCKY calculations find a moderately fast springback ($0.7 \mu\text{s}$ to twice the minimum radius and $0.15 \mu\text{s}$ to half the pressure) for the thin liner, in contrast to the significantly longer dwell time for the thick liner case. This behavior agrees substantially with SPW: they state that, for the 5 cm case, “the compressed target radius as well as profiles of the temperature, density and pressure at stagnation, and the evolution of pressure (deconfinement time) are practically identical to those for the 15 cm liner.”

The cumulative fusion energy yield and magnetic field vs. time are shown in Figure 12 for the 15 cm and 5 cm liner BUCKY 1-T calculations. The average mass density and ion energy in the target as a function of time for the 15 cm and 5 cm liner BUCKY 1-T calculations appear in Figure 13. As anticipated from theoretical considerations,^{18,23} the thinner liner produced a higher Q (fusion yield / input kinetic energy) than the thick liner. The input energy for the 15 cm case of 156 MJ, and yield of 0.36 MJ give $Q=0.002$, while the input energy for the 5 cm case of 44 MJ and yield of 1.3 MJ give $Q=0.03$. The magnitudes of these yields are consistent with theoretical expectations for DD or DT liners at these parameters; higher yields and Q s are predicted to require high-Z liners.¹⁸ The SPW results are that the 15 cm liner case gives $Q=0.012$ and the 5 cm case gives $Q=0.041$.

A two-temperature calculation for the 5 cm liner case appears to show a slightly longer dwell time than does the 1-T calculation based on the zone r-t plot, but the jet-target interface's radius and pressure evolution measures give nearly the same result (0.7 μ s to twice the minimum radius and 0.2 μ s to half the pressure). In general, the parameter evolution was analogous to the differences between the 1-T and 2-T results for the 15 cm liner case.

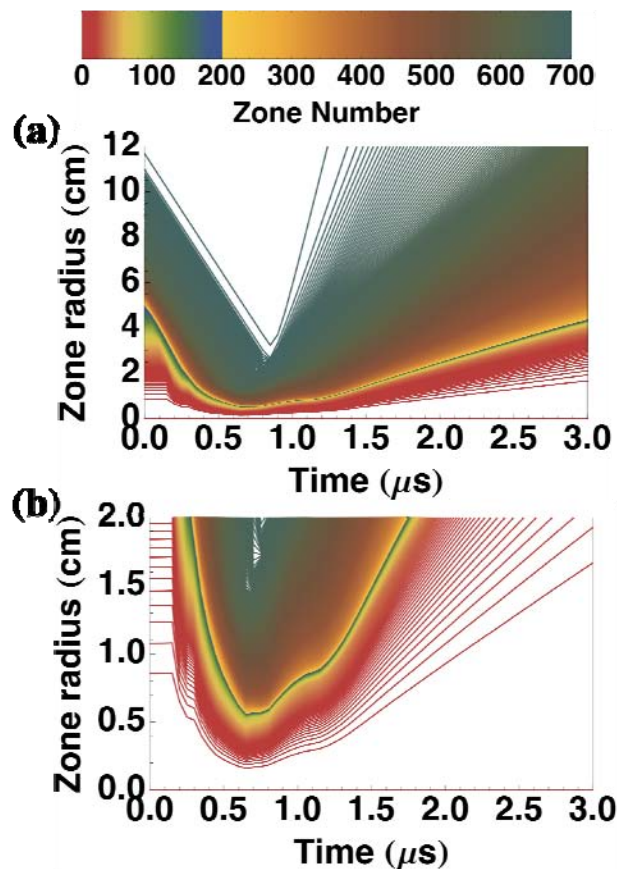


Figure 10. Lagrangian zone radii versus time for a 1-T BUCKY calculation showing (a) all zones and (b) the near-axis behavior of a case similar to the SPW 5 cm initial thickness liner case.

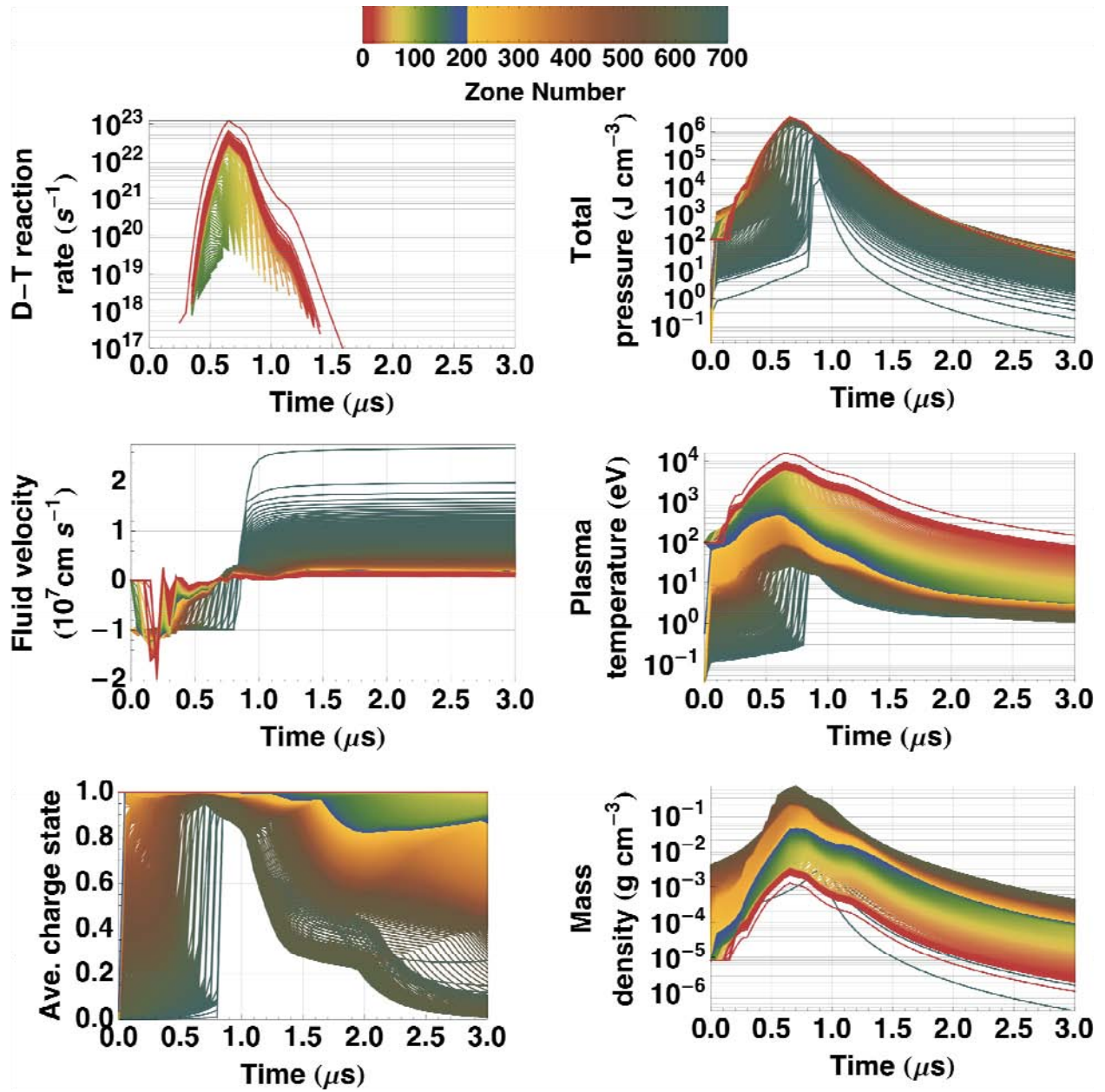


Figure 11. Selected zone parameters vs. time for the BUCKY DT plasma-jet MIF calculation of the 5 cm initial thickness liner case.

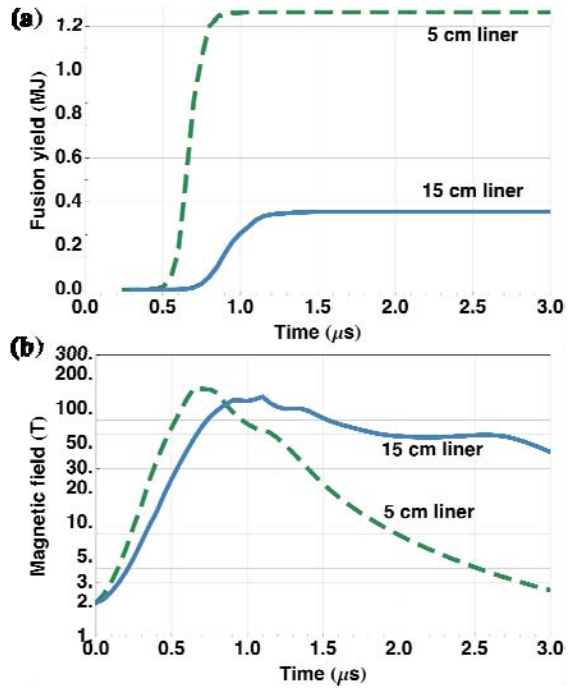


Figure 12. (a) Cumulative fusion energy yield and (b) magnetic field vs. time for 15 cm (solid blue) and 5 cm (dashed green) initial thickness liner BUCKY 1-T calculations.

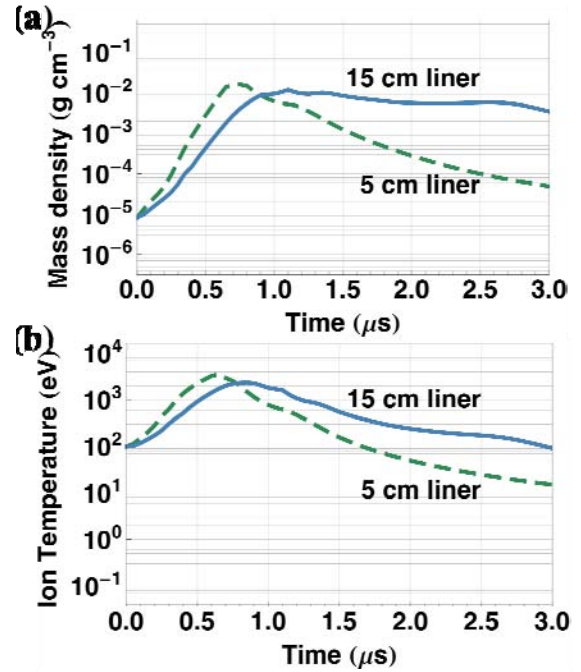


Figure 13. Average (a) mass density and (b) ion temperature vs. time for the target regions for 15 cm (solid blue) and 5 cm (dashed green) initial thickness liner BUCKY 1-T calculations.

V. CONCLUSIONS

Comparing the results of running the BUCKY code on Samulyak, Parks, and Wu's 15 cm initial thickness liner case²² with that paper's results supports some features of the SPW model, particularly during the early phase when the plasma jets converge toward the target. The dwell and expansion phases show significant differences, however, particularly in that the thick, massive liner increases the dwell time of near-maximum compression of the target much more in the BUCKY simulations than in Ref. 22. The thinner, 5 cm initial thickness liner case leads to a much faster springback of the compressed plasma, similar to the behavior of the Samulyak, et al. results and to typical inertial-confinement fusion (ICF) compression/expansion physics. The SPW paper states that the evolution of the pressure was practically identical for the 5 cm and 15 cm initial thickness liner cases, so this constitutes a significant difference between this paper's analysis and that of SPW.

Two-temperature calculations appear necessary for accurate calculations. The one-temperature calculations of both the present paper and Ref. 22 differ significantly from the present paper's two-temperature results.

The key conclusion of this paper is that magneto-inertial fusion physics possesses qualitatively different features from ICF physics, so the process of finding optimal solutions for high-yield target and plasma-jet parameters may require somewhat different approaches and analyses. These BUCKY results possess the encouraging feature that the long dwell time near stagnation at relatively high plasma density and temperature gives some confidence that optimizing the input parameters would generate cases that significantly increase the total fusion yield and Q . A future paper will treat optimization and parametric exploration.

ACKNOWLEDGMENTS

The author acknowledges useful conversations with G.A. Moses on radiation hydrodynamics and the BUCKY code. Valuable discussions on MIF physics were held with Y.C.F. Thio, D.D. Ryutov, P. Parks, and R. Samulyak. The conclusions of this paper are, however, solely the responsibility of the author. U.S. Department of Energy Grant DE-FG02-04ER54751 supported this research.

REFERENCES

- 1 R. Davidson, D. Arnett, J. Dahlburg, P. Dimotakis, D. Dubin, G. Gabrielse, D. Hammer, T. Katsouleas, W. Kruer, R. Lovelace, D. Meyerhofer, B. Remington, R. Rosner, A. Sessler, P. Sprangle, A. Todd, and J. Wurtele, *Frontiers in High Energy Density Physics: The X-Games of Contemporary Science* (National Academies Press, Washington, DC, 2003).
- 2 R. Davidson, T. Katsouleas, J. Arons, M. Baring, C. Deeney, L. DiMauro, T. Ditmire, R. Falcone, D. Hammer, W. Hill, B. Jacak, C. Joshi, F. Lamb, R. Lee, B.G. Logan, A. Mesissinos, D. Meyerhofer, W. Mori, M. Murnane, B. Remington, R. Rosner, D. Schneider, I. Silvera, J. Stone, B. Wilde, W. Zajc, and R. McKnight, *Frontiers for Discovery in High Energy Density Physics* (National Task Force on High Energy Density Physics, U.S. Office of Science and Technology Policy, Washington, DC, 2004).
- 3 D. Kovar, C.J. Keane, R. Dimeo, J.A. Morse, K. Beers, S.L. Ossakow, C. Deeney, A.A. Hauer, R.F. Schneider, F. Thio, E.A. Rohlving, M.P. Casassa, J. Simon-Gillo, R. Staffin, L.K. Len, M.H. Salaman, J.D. Gillaspay, T.B. Lucatorto, and J.L. Dehmer, *Report of the Interagency Task Force on High Energy Density Physics* (Interagency Working Group on the Physics of the Universe, National Science and Technology Council, 2007).
- 4 R. Betti, F. Beg, R. Davidson, P. Drake, R. Falcone, D. Hammer, M. Knudson, B.G. Logan, D. Meyerhofer, D.S. Montgomery, W. Mori, M. Murnane, R. Petrasso, B. Remington, D. Ryutov, J. Sethian, and R. Siemon, *Advancing the Science of High Energy Density Laboratory Plasmas* (Panel on High Energy Density Laboratory Plasmas, Fusion Energy Science Advisory Committee, Department of Energy, 2009).
- 5 R. Rosner and D. Hammer, *Basic Research Needs for High Energy Density Laboratory Physics* (Report of the Workshop on High Energy Density Laboratory Physics Research Needs, DOE SC and NNSA, 15-18 November 2009).
- 6 R.C. Kirkpatrick, I.R. Lindemuth, and M.S. Ward, "Magnetized Target Fusion: an Overview," *Fusion Technology* **27**, 201 (1995).
- 7 A.S. Bishop, *Project Sherwood* (Addison-Wesley, Reading, Massachusetts, 1958).
- 8 P.J. Turchi, ed., *Megagauss Physics and Technology* (Plenum, New York, 1980).
- 9 F.L. Ribe and A.R. Sherwood, "Fast-Liner-Compression Fusion Systems," in E. Teller, ed., in *Fusion, Volume 1, Part B* (Academic Press, New York, 1981).
- 10 I.R. Lindemuth and R.C. Kirkpatrick, "Parameter Space for Magnetized Fuel Targets in Inertial Confinement Fusion," *Nuclear Fusion* **23**, 263 (1983).
- 11 J.M. Taccetti, T.P. Intrator, G.A. Wurden, S.Y. Zhang, R. Aragonese, P.N. Assmus, C.M. Bass, C. Carey, S.A. deVries, W.J. Fienup, I. Furno, S.C. Hsu, M.P. Kozar, M.C. Langner, J. Liang, R.J. Maqueda, R.A. Martinez, P.G. Sanchez, K.F. Schoenberg, K.J. Scott, R.E. Siemon, E.M. Tejero, E.H. Trask, M. Tuszewski, W.J. Waganaar, C. Grabowski, E.L. Ruden, J.H. Degnan, T. Cavazos, D.G. Gale, and W. Sommars, "FRX-L: a Field-Reversed Configuration Plasma Injector for Magnetized Target Fusion," *Review of Scientific Instruments* **74**, 4314 (2003).
- 12 R.P. Drake, J.H. Hammer, C.W. Hartman, L.J. Perkins, and D.D. Ryutov, "Submegajoule Liner Implosion of a Closed Field Line Configuration," *Fusion Technology* **30**, 310 (1996).
- 13 R.C. Kirkpatrick and D.P. Smitherman, "Energetic Alpha Transport in a Magnetized Fusion Target," *Fusion Technology* **30**, 1311 (1996).

- 14 D.C. Barnes, "Scaling Relations for High-Gain, Magnetized Target Fusion Systems," *Comments on Plasma Physics and Controlled Fusion* **18**, 71 (1997).
- 15 J.H. Degnan, M.L. Alme, B.S. Austin, J.D. Beason, S.K. Coffey, D.G. Gale, J.D. Graham, J.J. Havranek, T.W. Hussey, G.F. Kiuttu, B.B. Kreh, F.M. Lehr, R.A. Lewis, D.E. Lileikis, D. Morgan, C.A. Outten, R.E. Peterkin, D. Platts, N.F. Roderick, E.L. Ruden, U. Shumlak, G.A. Smith, W. Sommars, and P.J. Turchi, "Compression of Plasma to Megabar Range using Imploding Liner," *Physical Review Letters* **82**, 2681 (1999).
- 16 G.A. Wurden, T. P. Intrator, D. A. Clark, R. J. Maqueda, J. M. Taccetti, F. J. Wysocki, S. K. Coffey, J. H. Degnan, and E. L. Ruden, "Diagnostics for a Magnetized Target Fusion Experiment," *Review of Scientific Instruments* **72**, 552 (2001).
- 17 T. Intrator, S.Y. Zhang, J.H. Degnan, I. Furno, C. Grabowski, S.C. Hsu, E.L. Ruden, P.G. Sanchez, J.M. Taccetti, M. Tuszewski, W.J. Waganar, and G.A. Wurden, "A High Density Field Reversed Configuration (FRC) Target for Magnetized Target Fusion: First Internal Profile Measurements of a High Density FRC," *Physics of Plasmas* **11**, 2580 (2004).
- 18 Y.C. F. Thio, E. Panarella, R.C. Kirkpatrick, C.E. Knapp, F. Wysocki, P. Parks, and G. Schmidt, "Magnetized Target Fusion in a Spheroidal Geometry with Standoff Drivers," in *Current Trends in International Fusion Research*, E. Panarella, ed. (NRC Press, National Research Council of Canada, Ottawa, Canada, 1999), p. 113.
- 19 Y.C.F. Thio, C.E. Knapp, R.C. Kirkpatrick, R.E. Siemon, and P.J. Turchi, "A Physics Exploratory Experiment on Plasma Liner Formation," *Journal of Fusion Energy* **20**, 1 (2002).
- 20 J.H. Degnan, W.L. Baker, M. Cowan, Jr., J.D. Graham, J.L. Holmes, E.A. Lopez, D.W. Price, D. Ralph, and N.F. Roderick, "Operation of Cylindrical Array of Plasma Guns," *Fusion Technology* **35**, 354 (1999).
- 21 F.D. Witherspoon, A. Case, S.J. Messer, R. Bomgardner, M.W. Phillips, S. Brockington, and R. Elton, "A Contoured Gap Coaxial Plasma Gun with Injected Plasma Armature," *Review of Scientific Instruments* **80**, 083506 (2009).
- 22 R. Samulyak, P. Parks, and L. Wu, "Spherically Symmetric Simulation of Plasma Liner Driven Magnetoinertial Fusion," *Physics of Plasmas* **17**, 092702 (2010).
- 23 P. Parks, "On the Efficacy of Imploding Plasma Liners for Magnetized Fusion Target Compression," *Physics of Plasmas* **15**, 062506 (2008).
- 24 R.R. Peterson, D.A. Haynes, I.E. Golovkin, and G.A. Moses, "Inertial Fusion Energy Target Output and Chamber Response: Calculations and Experiments," *Physics of Plasmas* **9**, 2287 (2002).; see also J.J. MacFarlane, G.A. Moses, and R.R. Peterson, *BUCKY-1—a 1-D Radiation Hydrodynamics Code for Simulating Inertial Confinement Fusion High Energy Density Plasmas*, University of Wisconsin Fusion Technology Institute Report UWFDM-984 (Madison, Wisconsin, 1995).
- 25 R.R. Peterson, J.J. MacFarlane, J.F. Santarius, P. Wang, and G.A. Moses, "The BUCKY and ZEUS-2D Computer Codes for Simulating High Energy Density ICF Plasmas," *Fusion Technology* **30**, 783 (1996).
- 26 T.A. Heltemes, E.P. Marriott, G.A. Moses, and R.R. Peterson, "Z-Pinch (LiF)₂-BeF₂ (Flibe) Preliminary Vaporization Estimation Using the BUCKY 1-D Radiation Hydrodynamics Code,"

- Twenty-First IEEE/NPSS Symposium on Fusion Engineering*, paper 10.1109/FUSION.2005.252866, pp. 1-4 (Knoxville, Tennessee, 26-29 September 2005).
- 27 G.A. Moses and J.F. Santarius, “High Energy Density Simulations for Inertial Fusion Energy Reactor Design,” *Fusion Science and Technology* **47**, 1121 (2005).
- 28 Ping Wang, “Computation and Application of Atomic Data for Inertial Confinement Fusion Plasmas,” University of Wisconsin Ph.D. thesis (1991).
- 29 S.I. Braginskii, “Transport Processes in a Plasma,” in *Reviews of Plasma Physics, Vol. 1* (Consultants Bureau, New York, 1965), p. 205.
- 30 O. V. Gotchev, D. D. Meyerhofer, O. Polomarov, R. Betti, P. Y. Chang, J. P. Knauer, J. A. Frenje, C. K. Li, M. J.-E. Manuel, R. D. Petrasso, F. H. Séguin, and J. R. Rygg, *LLE Review* **119**, 123 (2009).
- 31 Ping Wang, *Computation and Application of Atomic Data for Inertial Confinement Fusion Plasmas*, University of Wisconsin Ph.D. Thesis (1991).
- 32 J. Du, B. Fix, J. Glimm, X. Jia, X. Li, Y. Li, and L. Wu, “A Simple Package for Front Tracking,” *Journal of Computational Physics* **213**, 613 (2006).
- 33 R. Samulyak, J. Du, J. Glimm, and Z. Xu, , “A Numerical Algorithm for MHD of Free Surface Flows at Low Magnetic Reynolds Numbers,” *Journal of Computational Physics* **226**, 1532 (2007).
- 34 G. Kagan, X-Z. Tang, S.C. Hsu, and T.J. Awe, “Bounce-free Spherical Hydrodynamic Implosion,” *Physics of Plasmas* **18**, 120702 (2011).